2-3-2011

Pressure Distribution Over the Palm Region During Forward Falls on the Outstretched Hands

Woochol J. Choi
Chapman University, wchoi@chapman.edu

Stephen N. Robinovitch
Simon Fraser University

Recommended Citation

W.J. Choi, S.N. Robinovitch, Pressure distribution over the palm region during forward falls on the outstretched hands, Journal of Biomechanics, Volume 44, Issue 3, 3 February 2011, Pages 532-539, ISSN 0021-9290, http://dx.doi.org/10.1016/j.jbiomech.2010.09.011. (http://www.sciencedirect.com/science/article/pii/S0021929010004975)

Pressure Distribution Over the Palm Region During Forward Falls on the Outstretched Hands

Comments

Creative Commons License

Copyright

PubMed Central CANADA

Author Manuscript / Manuscrit d'auteur

J Biomech. Author manuscript; available in PMC 2012 October 15.

Published in final edited form as:

J Biomech. 2011 February 3; 44(3): 532–539. doi:10.1016/j.jbiomech.2010.09.011.

Pressure distribution over the palm region during forward falls on the outstretched hands

W.J. Choi[a,*] and **S.N. Robinovitch**[a,b]

[a]Injury Prevention and Mobility Laboratory, Department of Biomedical Physiology and Kinesiology, Simon Fraser University, Burnaby, BC, Canada V5A 1S6

[b]School of Engineering Science, Simon Fraser University, Burnaby, BC, Canada V5A 1S6

Abstract

Falls on the outstretched hands are the cause of over 90% of wrist fractures, yet little is known about bone loading during this event. We tested how the magnitude and distribution of pressure over the palm region during a forward fall is affected by foam padding (simulating a glove) and arm configuration, and by the faller's body mass index (BMI) and thickness of soft tissues over the palm region.

Thirteen young women with high (n=7) or low (n=6) BMI participated in a "torso release experiment" that simulated falling on both outstretched hands with the arm inclined either at 20° or 40° from the vertical. Trials were acquired with and without a 5 mm thick foam pad secured to the palm. Outcome variables were the magnitude and location of peak pressure (d, θ) with respect to the scaphoid, total impact force, and integrated force applied to three concentric areas, including "danger zone" of 2.5 cm radius centered at the scaphoid. Soft tissue thickness over the palm was measured by ultrasound.

The 5 mm foam pad reduced peak pressure, and peak force to the danger zone, by 83% and 13%, respectively. Peak pressure was 77% higher in high BMI when compared with low BMI participants. Soft tissue thickness over the palm correlated positively with distance (d) (R=0.79, p=0.001) and force applied outside the danger zone (R=0.76, p=0.002), but did not correlate with BMI (R=0.43, p=0.14). The location of peak pressure was shunted 4 mm further from the scaphoid at 20° than that of 40° falls (d=25 mm (SD 8), θ= −9° (SD 17) in the 20° falls versus d=21 mm (SD 8), θ= −5° (SD 24) in the 40° falls). Peak force to the entire palm was 11% greater in 20° compared with 40° falls.

These results indicate that even a 5 mm thick foam layer protects against wrist injury, by attenuating peak pressure over the palm during forward falls. Increased soft tissue thickness shunts force away from the scaphoid. However, soft tissue thickness is not predicted by BMI, and peak pressures are greater in high individuals than that of low BMI individuals. These results contribute to our understanding of the mechanics and prevention of wrist and hand injuries during falls.

*Corresponding author. Tel.: +1 778 782 6679; fax: +1 778 782 3040. woocholc@sfu.ca (W.J. Choi).

Conflict of interest statement

None of the authors above have any financial or personal relationships with other people or organizations that could inappropriately influence this work, including employment, consultancies, stock ownership, honoraria, paid expert testimony, patent applications/registrations, and grants or other funding.

Keywords

Colle's fracture; Scaphoid fracture; Wrist injury; Falls; Wrist guards; Impact angle; Body mass index; Soft tissue thickness; Biomechanics; Impact

1. Introduction

More than 97% of upper extremity fractures are the result of falls (Palvanen et al., 2000). Distal radius fractures are the most common type of fractures in young adults, and similar in frequency to hip fracture in older adults (Sahlin, 1990; Singer et al., 1998; O'Neill et al., 2001). The scaphoid is the most common carpal bone to be fractured, accounting for 60% of all carpal fractures (Hove, 1999). Wrist injuries represent 35–45% of all injuries among snowboarders and 37% among in-line skaters, and two thirds of those are fractures (Made and Elmqvist, 2004; Matsumoto et al., 2002; Schieber et al., 1996; Callé, 1994).

Previous studies have measured impact forces during falls on the outstretched hands. Chiu and Robinovitch (1998) reported that the hand impact force trace during this event is governed by a high-frequency peak force (F_{max1}) occurring shortly after the instant of contact, and a subsequent lower-frequency, lower magnitude peak (F_{max2}). These authors (Robinovitch and Chiu, 1998) also reported that F_{max1} was attenuated by 35% on average by a 1.3 cm thick foam rubber pad, nearly the same as the 40% attenuation provided by a 7.6 cm thick pad of the same material. The authors concluded that even a thin layer of padding, while having little effect on F_{max2}, may prevent wrist injuries during falls by substantially attenuating F_{max1}. DeGoede and Ashton-Miler (2002) showed that a fall arrest strategy involving elbow deflection reduced F_{max1} by 40% when compared with stiff-arm arrest. While these studies provide valuable insight on force magnitude, fracture risk depends also on distribution of force to the palm surface and underlying bones. To our knowledge, none of the previous study has reported these data.

The magnitude and distribution of contact force during a fall on the outstretched hands should also depend on the configuration of the body at impact, and soft tissue thickness over the palm region. While previous studies have examined the protective role of cadaveric soft tissue from the trochanteric hip region (Robinovitch et al., 1995), no study has examined the force-attenuating effect of palmar soft tissues.

In high risk activities (e.g., inline skating), hard-shell "wrist guards" are often used to reduce risk for fall-related distal radius fractures. While these splint-like devices undoubtedly reduce wrist hyperextension during impact (Schieber et al., 1996), epidemiological studies have reported contradictory results on clinical effectiveness (Lewis et al., 1997; Giacobetti et al., 1997; Hwang et al., 2006; Muller et al., 2003), or corresponding increases in the frequency of elbow, upper arm, and shoulder injuries—suggesting the need for improved design. Others have noted that the reduction in wrist flexibility created by hard-shell wrist guards makes them unsuitable for high risk activities such as bicycling, scootering, and use of playground equipment (Hagel et al., 2005; Cassell et al., 2005; Kim et al., 2006). Padded gloves or compliant floors represent alternative prevention strategies requiring investigation.

Accordingly, our goals in the current study were to conduct laboratory-based falling experiments to investigate how pressure distribution over the palm region during forward falls on the outstretched hands is affected by (1) a 5 mm thick foam pad, simulating a compliant surface or protective glove, (2) the impact angle of the arm, (3) the body mass index of the faller, and (4) the thickness of soft tissue over the palm region (as measured by ultrasound). Based on our results, we discuss potential applications to improved fracture prevention.

2. Methods

2.1. Subjects

Thirteen healthy young women between the age of 18 and 35 participated. Participants were selected so that approximately one-half (n=7) possessed a body mass index (BMI=weight/(height^2)) greater than 25, and the others (n=6) had a body mass index less than 18.5. Average body weight and height were 47 (SD 4) kg and 162 (SD 6) cm in the low BMI group, and 75 (SD 9) kg and 163 (SD 5) cm in the high BMI group. All participants provided written informed consent. The experimental protocol and consent form were approved by the Committee on Research Ethics at Simon Fraser University.

2.2. Equipment

During each trial, we collected total hand impact force from a force plate (Bertec, USA) and pressure distribution from a 2D scanning plate (RSscan International, Belgium) placed on the force plate, at 500 Hz of sampling rate. Reflective markers were placed on the dorsal surface of each hand, directly over the scaphoid, hamate, 2nd metacarpal head, and 5th metacarpal head (identified by palpation). The 3D positions of these markers were recorded at 250 Hz with an eight-camera video-based motion measurement system (Motion Analysis Corp., USA).

2.3. Protocol

Forward falls were simulated through “torso release experiments,” which involved releasing the participant (via a tether and electromagnet) from a state of impending impact with the palm raised 5 cm above the ground (see Chiu and Robinovitch (1998) for further details). To assess the effect of impact configuration on contact force and pressure, trials were acquired for initial inclinations of the arm from the vertical of 20° and 40° (Fig. 1). Given the brief interval between tether release and impact, negligible changes occurred during descent in the relative positions of the arm, forearm and hand, as confirmed during the trials through visual monitoring by one of the investigator, and later by review of video footage acquired for each trial. Trials were also conducted without a pad and with a 5 mm thick ethylene vinyle acetate (EVA) foam pad (13 × 21 cm; density of 46.6 kg/m^3; see inset in Fig. 1), which was placed on the palm by means of double sided tape. Three trials were acquired for each condition. The order of presentation of the conditions was randomized.

2.4. Data analysis

Our main outcome variables were the magnitude of peak pressure, location of peak pressure, total peak force, and integrated force applied to each of three defined palm regions. Except for the total peak force, each of these variables were calculated for the right and left hand separately, and then averaged for analysis (Troy and Grabiner, 2007). Data analysis was conducted with customized Matlab routines. The magnitude of peak pressure was determined by the peak value from the pressure versus time trace, where the maximum pressure values from 4096 pressure sensors in the RSscan plate were plotted as a function of time. The location of peak pressure with respect to the scaphoid was expressed by the angle (θ) from the line between scaphoid and hamate, and the distance (d) from the scaphoid (Fig. 2d). The magnitude of peak total force was taken as the peak value in the vertical force trace during impact (Fig. 2a and b).

We defined three regions over the palm: area A – a circle of 5 cm diameter, centered at the scaphoid, area B – an adjacent 2 cm wide donut shape and area C – the remainder of the palm region (Fig. 2d). We refer to area A as the ‘danger zone’ because it covers the scaphoid and lunate, which articulate with and transmit force to the distal radius (Calais-Germain, 1993). Thus, force to the danger zone affects risk for distal radius (Colles’) fracture, and

scaphoid and lunate fracture. We calculated the integrated force applied to each region as the sum of all pressure values measured by the corresponding sensors multiplied by the area of the each defined region, and computed percent force defined by the ratio of the region's integrated force to total integrated force. To determine an anatomical mapping of pressure applied to the entire palm region, we transformed the coordinate system of the M.A.C. motion measurement system into that of the pressure data from RSscan. This allowed us to estimate the location of the scaphoid, hamate, 2nd metacarpal head, 5th metacarpal head, and orientation of the hand on the RSscan map of pressure distribution (Fig. 3).

We measured participants' soft tissue thickness, directly over the scaphoid and hamate hook, using an ultrasound machine (Acuson Antares, Siemens Inc., Germany). During the scans, we palpated target bones, confirmed the spot by ultrasound image, and then recorded. The ultrasound probe carefully contacted the skin, ensuring the same pressure and angle was applied across all subjects. Both hands were scanned and averaged for data analysis.

Repeated measures ANOVA was used to test whether our outcome variables were associated with pad condition (2 levels), impact configuration (2 levels), and BMI (2 levels). The Pearson correlation test was used to test relationships between soft tissue thickness over the palm and each outcome variables. In one set of analysis, we used raw magnitudes of peak force and distance. In a second set of analysis, we normalized our outcome variables (by dividing force by body weight (N), and distance by body height (m)) to facilitate comparison between high and low BMI groups, and based on the consideration that bone fracture force will tend to scale with body size. All analyses were conducted with the SPSS 16.0, using a significance level of α=0.05.

3. Results

The magnitude of peak pressure associated with pad condition (F=22.2, p=0.001) and BMI (F=7.3, p=0.02), but not with impact configuration (F=2.6, p=0.131), and there were no interaction effects. Peak pressure was reduced to 83% by the pad (from 616 to 336 kPa), and was 77% higher in high BMI than in low BMI individuals (608 kPa versus 344 kPa) (Fig. 4).

Peak force to the entire palm region associated with impact configuration (F=41.3, p=0.0005) and BMI (F=29.4, p=0.0005), but not with pad condition (F=1.1, p=0.29), and there were no interaction effects. Peak force was 12% greater in the 20° fall than in the 40° fall configuration (486 N versus 431 N), and 47% greater in high BMI than in low BMI individuals (547 N versus 371 N). The normalized peak force associated with impact configuration (F=34.7, p=0.0005) only, and there were no interactions. The normalized peak force was 11% greater in the 20° fall than in the 40° fall configuration (816 versus 732) (Table 1).

The location of peak pressure associated with impact configuration (distance only; distance F=5.8, p=0.034, distance normalized F=5.9, p=0.032, angle F=3.2, p=0.099), but not with pad condition (distance F=1.17, p=0.302, angle F=2.7, p=0.128) and BMI (distance F=2.61, p=0.134, angle F=0.02, p=0.885), and there were no interaction effects. Peak pressure occurred at 25 mm from the scaphoid and −9° from the line between scaphoid and hamate in the 20° fall configuration, and 21 mm from the scaphoid and −5° from the scaphoid-hamate axis in the 40° fall configuration (Fig. 5).

The integrated force on the danger zone associated with pad condition (F=6.5, p=0.027), and BMI (F=16.5, p=0.002), but not with impact configuration (F=4.4, p=0.059), and there were no interactions. The force on the danger zone was reduced 13% by the pad (from 94 N to 83 N), and was 90% greater in high BMI than in low BMI individuals (116 N versus 61 N). The normalized force on the danger zone associated with the pad condition (F=6.9, p=0.023)

decreases 15% (from 156 to 136), but not with impact configuration (F=4.1, p=0.06) and BMI (F=1.2, p=0.285), and there were no interactions (Fig. 6a, b, and c). The percent of total force applied to the danger zone, on average, ranged from 39–46%, and was reduced by padding (p=0.023), but was not altered by impact configuration or BMI (Fig. 6d). In addition, the normalized force on area B associated with impact configuration (F=10.3, p=0.008) and BMI (F=8.6, p=0.014), averaging 23% greater in the 20° fall configuration compared with 40° fall configuration, and 54% greater in the high BMI than in low BMI group, but not with pad condition (F=0.008, p=0.92). Conversely, the normalized force on area C associated with pad condition (F=19.9, p=0.001) and impact configuration (F=18.2, p=0.001), averaging 47% greater in the padded condition and 42% greater in the 20° fall configuration compared with 40° fall configuration, but not with BMI (F=3.2, p=0.97).

Soft tissue thickness over the scaphoid positively correlated with distance (R=0.79, p=0.001), and normalized force applied to area C (R=0.76, p=0.002), but not with peak pressure, peak force, force applied to danger zone and to area B, and BMI. Similar trends were observed for soft tissue thickness over the hamate.

4. Discussion

In this study, we conducted laboratory experiments to measure the distribution of pressure applied to the palm during forward falls onto the outstretched hands, and to determine how pressure distribution depends on foam padding (simulating a glove), the impact angle of the arm, the body mass index of the faller, and the thickness of soft tissue over the palm region.

We found that in the 5 mm thick pad we tested caused substantial attenuation in peak pressure, but had little effect on peak total force. On average, the pad reduced peak pressure by 83%, and peak force to the “danger zone” centered at the scaphoid by 13%. However, it had no effect on peak total force applied to the entire palm, and location of peak pressure. This suggests that the pad altered local variation in stiffness over the palm, but not total effective stiffness. These findings agree with our recently reported results (Choi et al., 2010) that a soft shell hip protector reduced peak pressure, but not peak force, during simulated sideways falls on the hip (“pelvis release experiments”).

We also found that peak pressure over the palm associated significantly with BMI, with 77% greater values observed in the high BMI than in the low BMI group. This finding is consistent with our observation of higher raw magnitudes of peak force applied to the entire palm region in high than in the low BMI individuals, and with our observation of no association between BMI and ultrasound measures of the thickness of soft tissue overlying the scaphoid or hamate—a variable that we presumed would mediate the effect of BMI on peak pressure. Interestingly, these findings contrast with our recently reported results for simulated falls on the hip region (“pelvis release experiments”) with the same subjects (Choi et al., 2010), where peak pressure over the greater trochanter averaged 266% higher in low BMI than in high BMI participants. The likely explanation for this discrepancy is the site-specific nature of the association between BMI and soft tissue thickness. In particular, in our participants, soft tissue thickness over the greater trochanter averaged 23 mm larger in high BMI than in low BMI individuals (46.8 mm versus 23.8 mm). However, tissue thickness over the scaphoid differed between groups by less than 1 mm (7.7 mm in high BMI versus 6.9 mm in low BMI individuals). Thus, individuals with high BMI benefit from the cushioning effect of thicker soft tissue over the hip (which offsets the effect of increased body mass), but no such benefit exists for falls on the outstretched hands, where tissue thickness is relatively uniform.

In addition to load magnitude, fracture risk during a fall will depend on the point of load application. Our results suggest that arm configuration affects each of these parameters. In

particular, we found that the location of peak pressure tends to be near the periphery of the "danger zone", along a line just slightly below (by 7°) the scaphoid-hamate axis, and at an average distance from the scaphoid, which was 19% larger in the 20° fall configuration than in the 40° fall configuration (25 versus 21 mm). Neither padding nor BMI affected the location of peak pressure. Several authors have discussed that bending stresses likely contribute to Colles' fracture (Dobyns and Linscheid, 1984; Myers et al., 1991). Since the scaphoid is directly aligned and transmits compressive force to the distal end of the radius, it is reasonable to regard our peak pressure distances as representative of the moment arm between the distal end of the radius and the center of vertical force application. Our results then suggest that peak stresses at the distal radius will be higher in a 20° fall configuration than in a 40° fall configuration for two reasons: a 19% larger moment arm, and an 11% increase in normalized peak force.

There are several limitations to this study. We examined only one type of padding as a preliminary assessment of the protective value of wearable gloves, and as discussed further below, future studies should examine systematically how glove geometry and material influence our outcome variables. Our sample size (of 13 participants) was relatively modest, and additional experiments with a larger sample are warranted, especially to confirm our findings regarding the associations between BMI, palmar soft tissue thickness, and peak pressure during impact. Due to safely reasons, our fall height was limited to 5 cm. However, this was sufficient to produce peak vertical forces averaging 590 N, close to the peak forces reported for more realistic fall conditions, found by Degoede and Ashton-Miller (2002) to average 611 (SD 141) N, and by Lo at al. (2003) to average 758 (SD 144) N. This observation supports the clinical relevance of our findings. Also, we focused on a specific, worst case fall scenario, by instructing participants to maintain their elbows extended throughout impact (DeGoede and Ashton-Miler, 2002). However, we can think of little reason why our observed trends would not also apply for falls involving elbow flexion during impact. Finally, we examined only vertical forces and pressure distribution, and not horizontal shear forces applied to the palm. Future studies should seek to determine the relative contribution of vertical versus horizontal force to fracture risk during a fall, and how factors such as padding, surface friction, impact configuration, and BMI affect horizontal forces.

Encouraged by our current results, future studies should focus on the systematic evaluation of a wider range of energy-absorbing gloves, and compliant floors as an alternative to rigid wrist guards in preventing fall-related wrist injuries. We found that, even in our padded condition, at least 39% of total force is applied to the "danger zone" directly overlying the scaphoid and hamate (and will, in turn, be transmitted to the distal radius), and an interesting question is whether gloves can be designed to reduce this value substantially. Several types of marketed gloves incorporate foam that varies over the palm in thickness and/or density, and these warrant testing as a first step in addressing this issue. Similarly, along with its traditional role in playground design, compliant flooring is emerging as a feasible option for preventing hip fractures in high risk environments for older adults (Laing and Robinovitch, 2009), and studies should further assess the clinical and biomechanical benefit of these products in attenuating and re-distributing impact force and risk for fall-related wrist injuries (Robinovitch and Chiu, 1998).

Acknowledgments

This research was supported in part by a Discovery Grant from the Natural Science and Engineering Research Council of Canada (RGPIN 239735) to SNR.

References

Callé SC. In-line skating injuries, 1987 through 1992. American Journal of Public Health. 1994; 84:675.

Calais-Germain, B. Anatomy of Movement. 1. Eastland Press; Seattle WA: 1993. p. 150

Cassell E, Ashby K, Gunatilaka A, Clapperton A. Do wrist guards have the potential to protect against wrist injuries in bicycling, micro scooter riding, and monkey bar play? Injury Prevention. 2005; 11(4):200–203. [PubMed: 16081745]

Chiu J, Robinovitch SN. Prediction of upper extremity impact forces during falls on the outstretched hand. Journal of Biomechanics. 1998; 31 (12):1169–1176. [PubMed: 9882050]

Choi WJ, Hoffer JA, Robinovitch SN. Effect of hip protectors, falling angle and body mass index on pressure distribution over the hip during simulated falls. Clinical Biomechanics. 2010; 25 (1):63–69. [PubMed: 19766363]

DeGoede KM, Ashton-Miler JA. Fall arrest strategy affects hand impact force in a forward fall. Journal of Biomechanics. 2002; 35:843–848. [PubMed: 12021005]

Dobyns, JH.; Linscheid, RL. Fractures and dislocations of the wrist. In: Rockwood, CA.; Green, DP., editors. Fractures in Adults. JB Lippincott Co; Philadelphia: 1984.

Giacobetti FB, Sharkey PF, Bos-Giacobetti MA, Hume EL, Taras JS. Biomechanical analysis of the effectiveness of in-line skating wrist guards for preventing wrist fractures. American Journal of Sports Medicine. 1997; 25 (2):223–225. [PubMed: 9079178]

Hagel B, Pless IB, Goulet C. The effect of wrist guard use on upper-extremity injuries in snowboarders. American Journal of Epidemiology. 2005; 162 (2):149–156. [PubMed: 15972933]

Hove LM. Epidemiology of scaphoid fractures in Bergen, Norway. Scandinavian Journal of Plastic and Reconstructive Surgery and Hand Surgery. 1999; 33 (4):423–426. [PubMed: 10614752]

Hwang IK, Kim KJ, Kaufman KR, Cooney WP, An KN. Biomechanical efficiency of wrist guards as a shock isolator. Journal of Biomechanical Engineering. 2006; 128 (2):229–234. [PubMed: 16524335]

Kim KJ, Alian AM, Morris WS, Lee YH. Shock attenuation of various protective devices for prevention of fall-related injuries of the forearm/hand complex. American Journal of Sports Medicine. 2006; 34 (4):637–643. [PubMed: 16382013]

Laing AC, Robinovitch SN. Low stiffness floors can attenuate fall-related femoral impact forces by up to 50% without substantially impairing balance in older women. Accident Analysis and Prevention. 2009; 41 (3):642–650. [PubMed: 19393817]

Lewis LM, West OC, Standeven J, Jarvis HE. Do wrist guards protect against fractures? Annals of Emergency Medicine. 1997; 29(6):766–769. [PubMed: 9174522]

Lo J, McCabe GN, DeGoede KM, Okuizumi H, Ashton-Miller JA. On reducing hand impact force in forward falls: results of a brief intervention in young males. Clinical Biomechanics. 2003; 18 (8): 730–736. [PubMed: 12957559]

Made C, Elmqvist LG. A 10 year study of snowboard injuries in Lapland Sweden. Scandinavian Journal of Medicine and Science in Sports. 2004; 14:128–133. [PubMed: 15043635]

Matsumoto K, Miyamoto K, Sumi H, Sumi Y, Shimizu K. Upper extremity injuries in snowboarding and skiing: a comparative study. Clinical Journal of Sport Medicine. 2002; 12:354–359. [PubMed: 12466690]

Müller I, Vogiatzis M, Wiese K, Sönnichsen S, Zantop T, Oehlert K, Petersen W, Hassenpflug J. Biomechanical examinations of the efficacy of wrist guards in inline skating. Sportverletz Sportschaden. 2003; 17(2):80–83. German. [PubMed: 12817320]

Myers ER, Sebeny EA, Hecker AT, Corcoran TA, Hipp JA, Greenspan SL, Hayes WC. Correlations between photon absorption properties and failure load of the distal radius in vitro. Calcified Tissue International. 1991; 49 (4):292–297. [PubMed: 1760774]

O'Neill TW, Cooper C, Finn JD, Lunt M, Purdie D, Reid DM, Rowe R, Woolf AD, Wallace WA, Colles UK. Fracture Study Group. Incidence of distal forearm fracture in British men and women. Osteoporosis International. 2001; 12 (7):555–558. [PubMed: 11527052]

Palvanen M, Kannus P, Parkkari J, Pitkajarvi T, Pasanen M, Vuori I, Jarvinen M. The injury mechanisms of osteoporotic upper extremity fractures among older adults: a controlled study of

287 consecutive patients and their 108 controls. Osteoporosis International. 2000; 11 (10):822–831. [PubMed: 11199185]

Robinovitch SN, Chiu J. Surface stiffness affects impact force during a fall on the outstretched hand. Journal of Orthopaedic Research. 1998; 16 (3):309–313. [PubMed: 9671925]

Robinovitch SN, McMahon TA, Hayes WC. Force attenuation in trochanteric soft tissues during impact from a fall. Journal of Orthopaedic Research. 1995; 13 (6):956–962. [PubMed: 8544034]

Sahlin Y. Occurrence of fracture in a defined population: a 1-year study. Injury. 1990; 21 (3):158–160. [PubMed: 2401547]

Schieber RA, Branche-Dorsey CM, Ryan GW, Rutherford GW Jr, Stevens JA, O'Neil J. Risk factors for injuries from in-line skating and the effectiveness of safety gear. New England Journal of Medicine. 1996; 335 (22):1630–1635. [PubMed: 8929359]

Singer BR, McLauchlan GJ, Robinson CM, Christie J. Epidemiology of fractures in 15,000 adults: the influence of age and gender. Journal of Bone and Joint Surgery [British]. 1998; 80 (2):243–248.

Troy KL, Grabiner MD. Asymmetrical ground impact of the hands after a trip-induced fall: experimental kinematics and kinetics. Clinical Biomechanics. 2007; 22 (10):1088–1095. [PubMed: 17888549]

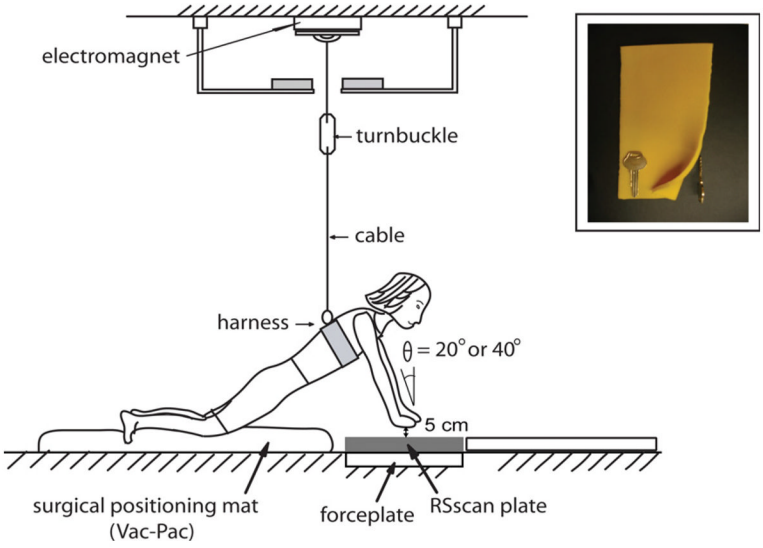

Fig. 1.

Schematic of the "torso release experiment". In some trials, we placed a 5 mm thick layer of EVA foam (13 × 21 cm, density of 46.6 kg/m^3) over the palmar surface, as shown in the inset. Surgical positioning mats (Vac-Pac, Olympic Medical, Seattle, WA, USA) were placed under the knee, shin, and foot to ensure consistent positioning of the participant between successive trials in a given impact configuration.

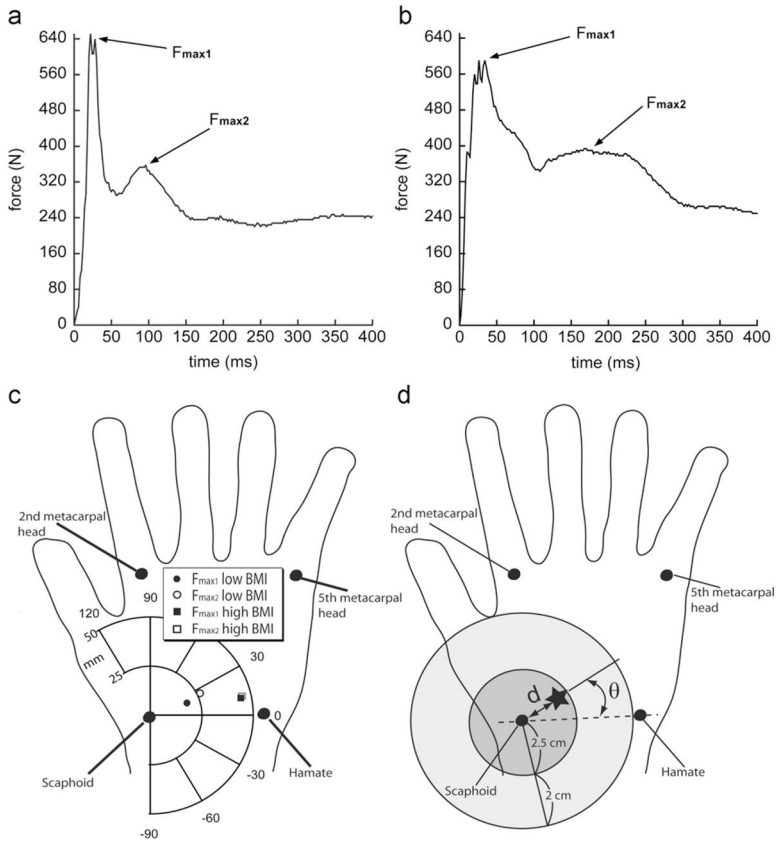

Fig. 2.

Techniques for analyzing pressure data. Raw force traces (shown in (a) from a low BMI participant and in (b) from a high BMI participant) tended to exhibit two successive peaks in force (F_{max1} and F_{max2}). (c) The locations of peak pressure corresponding to the instants of F_{max1} and F_{max2} from the same sample trials. (d) The location of peak pressure was expressed as the distance (d) from the scaphoid and angle (θ) from the line between scaphoid and hamate. Three different areas were defined over the palm region: area A (danger zone, dark gray) comprised a circle of 5 cm diameter centered at the scaphoid; area B (light gray) was an adjacent donut shape of 9 cm outer diameter and 5 cm inner diameter centered at the scaphiod; and area C (white) consisted of the remainder of the palm region.

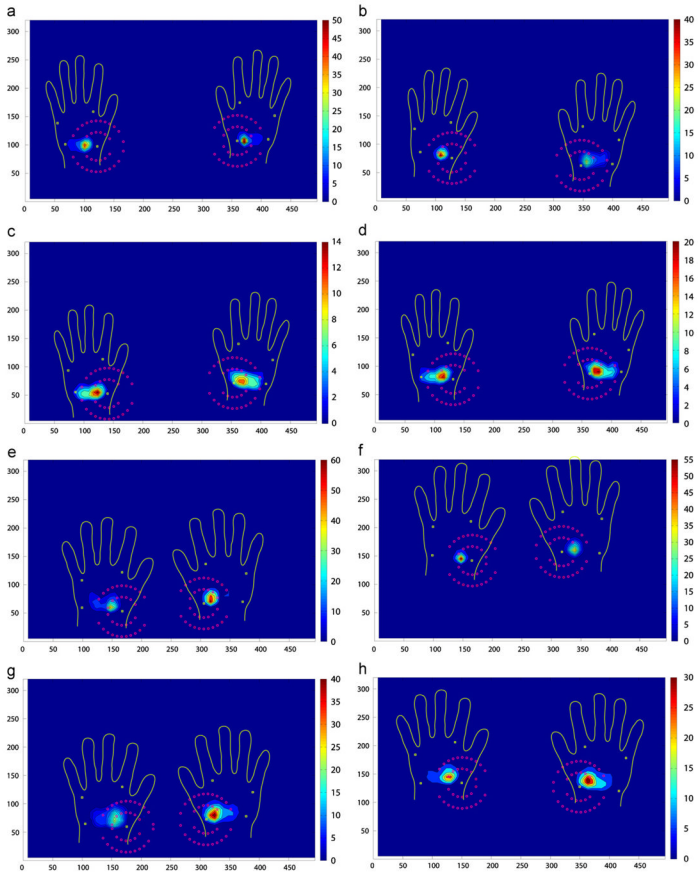

Fig. 3.

Typical pressure profiles from trials in each condition. In general, the peak pressure was located between the scaphoid and hamate, with the contact area increasing, and the peak pressure decreasing, in the padded (versus unpadded) condition. (a) Low BMI, unpadded 20° fall, (b) low BMI, unpadded 40° fall, (c) low BMI, padded 20° fall, (d) low BMI, padded 40° fall, (e) high BMI, unpadded 20° fall, (f) high BMI, unpadded 40° fall, (g) high BMI, padded 20° fall, (h) high BMI, padded 40° fall. In (a)–(h), the magnitude of pressure is indicated by a color scale, which can be interpreted by referring to the color bar legend at the right of each figure, showing units of N/cm^2 (1 N/cm^2=10 kPa). Note the differences between the figures in the displayed pressure range.

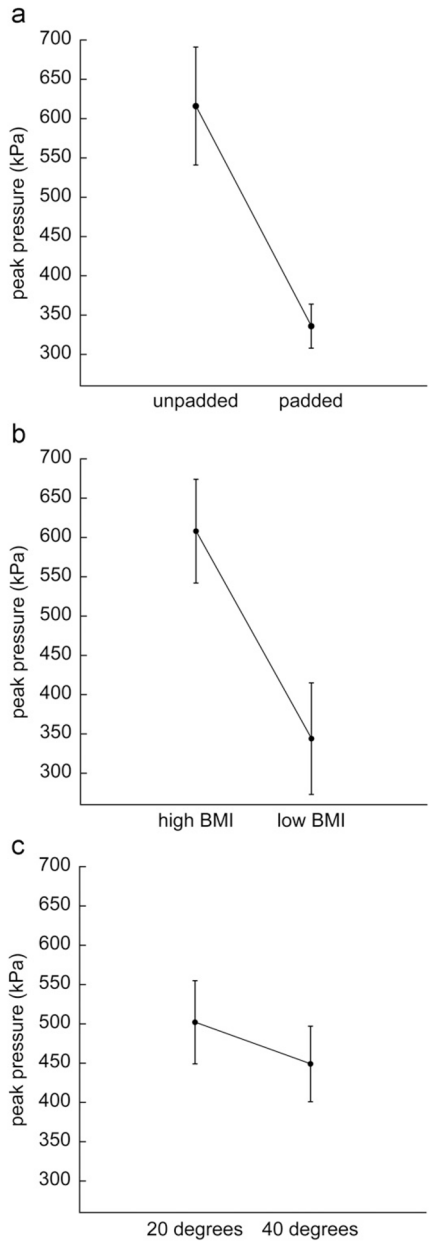

Fig. 4.

Effect of the 5 mm thick EVA foam pad, BMI and impact configuration on the magnitude of peak pressure over the palm region. (a) The pad significantly reduced peak pressure (p=0.001). (b) Peak pressure was greater in high BMI than in low BMI participants (p=0.02). (c) There was no significant effect of impact configuration on peak pressure (p=0.131).

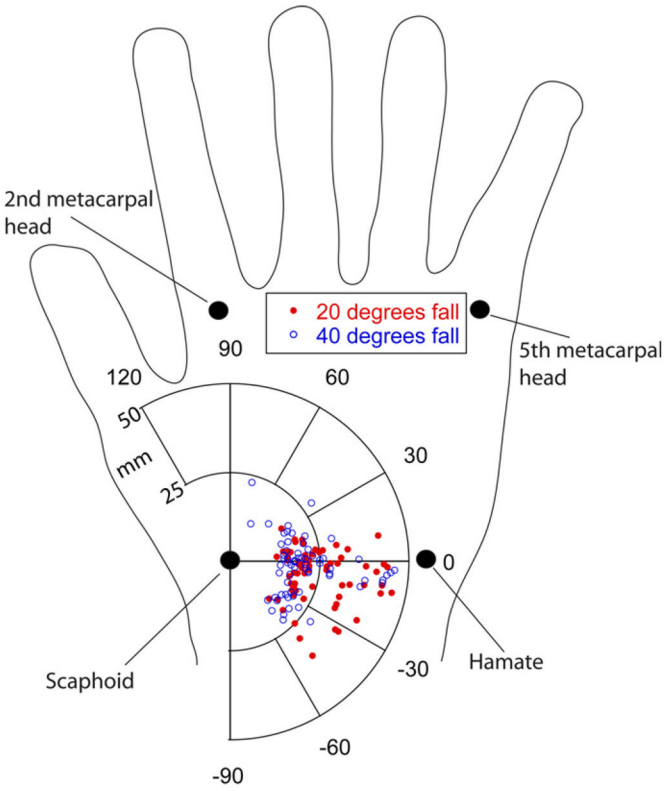

Fig. 5.
Location of peak pressure. Each data point represents an individual trial in each condition across all subjects. The average location of peak pressure was 25 (SD 8) mm from the scaphoid and −9 (SD 17) deg. from the line between scaphoid and hamate in the 20° fall, and 21 mm (SD 8) mm from the scaphoid and −5 (SD 24) deg. in the 40° fall.

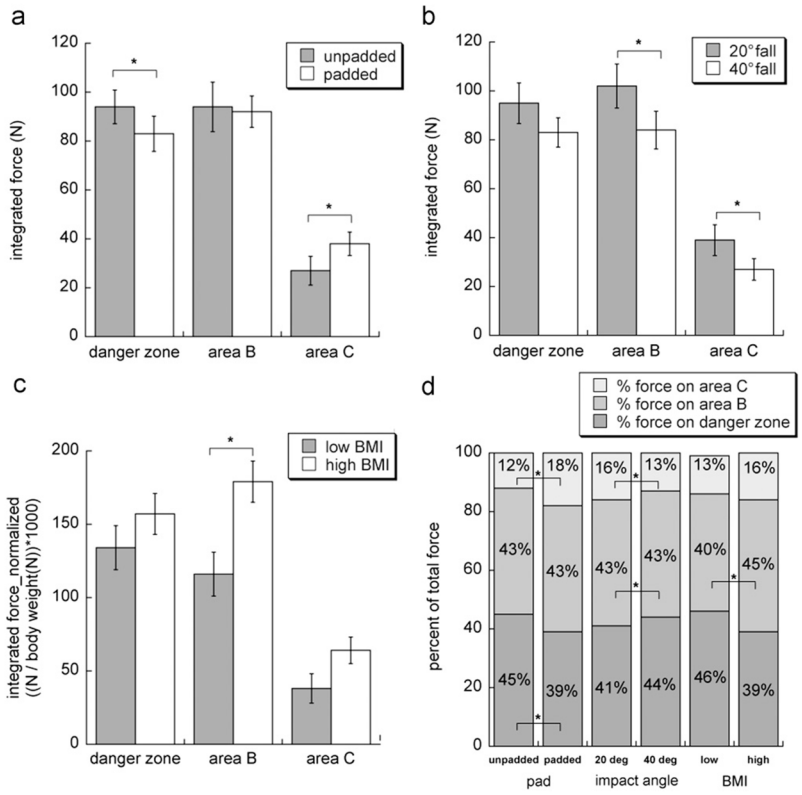

Fig. 6.

Force distribution over the three defined areas of the palm. (a) Unpadded versus padded. (b) 20° versus 40° fall configuration. (c) Low versus high BMI. (d) Percent force applied to each area. For example, 45% of total force was applied to the danger zone, and 43% and 12% of total force were applied to area *B* and *C*, respectively, in the unpadded condition. Note that data were normalized by body weight (*N*) before conducting statistical analysis, and an asterisk indicates statistical significance ($p<0.05$).

Table 1

Mean parameter values in each condition (with standard errors shown in parentheses).

Variable	20° falls				40° falls			
	high BMI		low BMI		high BMI		low BMI	
	Unpadded	Padded	Unpadded	Padded	Unpadded	Padded	Unpadded	Padded
	n=7	n=7	n=6	n=6	n=7	n=7	n=6	n=6
Peak pressure								
kPa	808 (108)	432 (44)	515 (117)	254 (48)	748 (104)	444 (56)	392 (112)	214 (61)
Peak force (F_{max1})								
N	590 (26)	584 (25)	379 (28)	392 (27)	498 (21)	515 (20)	356 (22)	356 (21)
N/BW[a] × 1000	799 (27)	794 (30)	822 (29)	850 (33)	677 (26)	701 (27)	777 (28)	772 (29)
Distance, peak pressure (d)								
mm	27.3 (2.7)	28.7 (2.8)	22.2 (2.9)	22.0 (3.0)	23.6 (2.3)	25.1 (2.5)	18.6 (2.5)	19.5 (2.7)
mm/BH[b] × 1000	16.7 (1.6)	17.5 (1.7)	13.7 (1.8)	13.6 (1.8)	14.5 (1.5)	15.4 (1.6)	11.5 (1.6)	12.0 (1.7)
Angle, peak pressure (θ)								
Degrees	−9 (6)	−6 (7)	−13 (6)	−8 (7)	−6 (8)	−2 (8)	−7 (9)	−3 (8)
Force on the danger zone								
N	132 (12)	116 (11)	74 (13)	56 (12)	110 (8.3)	107 (10)	61 (9)	54 (10)
N/BW[a] × 1000	179 (22)	156 (16)	162 (24)	123 (18)	150 (15)	145 (14)	133 (17)	118 (15)
Force on area B								
N	157 (16)	128 (10)	61 (17)	65 (11)	120 (14)	125 (11)	41 (15)	51 (12)
N/BW[a] × 1000	212 (23)	172 (12)	131 (24)	139 (13)	163 (20)	171 (18)	88 (21)	108 (19)
Force on area C								
N	55 (11)	58 (7)	19 (12)	24 (7)	27 (6)	52 (7)	8 (6)	21 (8)
N/BW[a] × 1000	72 (14)	78 (10)	40 (15)	51 (11)	36 (8)	70 (11)	17 (9)	45 (12)

[a] Peak forces are normalized by body weight (BW).

[b] Distances are normalized by body height (BH).